

ROD-CLIMBING IN MOLTEN POLYMERS

by

VU Thi Khanh Phuong

**Submitted to the Faculty of Graduate Studies and Research
of McGill University in Partial Fulfillment
of the Requirements for the
Degree of Master of Engineering**

Thesis Supervisor: Professor John M. Dealy

**Department of Chemical Engineering
McGill University
Montreal, Canada**

March 1976

ROD-CLIMBING IN MOLTEN POLYMERS

VU Thi Khanh Phuong

Department of Chemical Engineering

A well-known curiosity in the field of experimental rheology is the tendency of viscoelastic liquids to rise up on the surface of a cylinder rotating in a large container of the liquid. This phenomenon is usually referred to as "rod-climbing" or the "Weissenberg effect." Recently, several experimental and theoretical studies on this phenomenon have been made. However, experimental results to date have been limited to polymer solutions.

In the present study, an apparatus has been designed and constructed to study the "Weissenberg effect" in molten polymers. Three commercial polyethylene resins were studied: one high density polyethylene (HDPE) at 190°C, and two low density polyethylenes (LDPE) at 182°C. For each resin, the variation of the height of rise with the angular velocity was determined: for the HDPE, the height varies linearly with the velocity, for one LDPE, the height is proportional to the square of the angular velocity. For the two LDPE resins, curves of height of rise versus time were obtained, and it was observed that at higher speeds, after a fairly rapid increase, the height leveled off for a period of time, then increased again until a second steady state value was reached. The resin which had the highest viscosity and lowest density gave the greatest height of rise.

L'EFFET WEISSENBERG DANS LES POLYMÈRES FONDUS

VU Thi Khanh Phuong

Département de Génie Chimique

Un fait curieux bien connu dans le domaine de rhéologie expérimentale est la tendance des liquides viscoélastiques de grimper à la surface d'un cylindre tournant dans un grand récipient de liquide. Ce phénomène est communément appelé l'"Effet Weissenberg". Récemment, plusieurs études expérimentales et théoriques sur ce phénomène ont été réalisées. Cependant, les résultats expérimentaux jusqu'à ce jour ont été limités aux solutions de polymère.

Dans la présente étude, un montage expérimental a été conçu et construit pour étudier l'"Effet Weissenberg" dans les polymères fondus. Trois résines commerciales de polyéthylène ont été étudiées: une de haute densité à 190°C et deux de basse densité à 182°C. La variation de la hauteur de montée pour chaque résine a été déterminée en fonction de la vitesse angulaire: il a été observé que, pour le polyéthylène de haute densité, cette hauteur varie linéairement avec la vitesse, tandis que pour un des deux polyéthylènes de basse densité, la hauteur de montée est proportionnelle au carré de la vitesse angulaire. On a reporté les valeurs de la hauteur de montée en fonction du temps et on a observé que pour les grandes vitesses, après une assez rapide augmentation, la hauteur se stabilise pendant un certain temps, puis remonte à nouveau jusqu'à atteindre une seconde valeur stationnaire. La résine qui a la plus grande viscosité et la plus basse densité accuse la plus haute montée.

ACKNOWLEDGEMENTS

I would like to express my sincere gratitude to:

my research director, Professor J.M. Dealy, for his support and encouragement throughout the course of this work;

the staff of the Chemical Engineering Department electronic and machine shops, particularly Mr. B. Hoogendoorn, Mr. A. Krish and Mr. T. Wartenbergh for their help in designing and constructing the apparatus; and

my parents and my brother for their moral support.

ABSTRACT

A well-known curiosity in the field of experimental rheology is the tendency of viscoelastic liquids to rise up on the surface of a cylinder rotating in a large container of the liquid. This phenomenon is usually referred to as "rod-climbing" or the "Weissenberg effect." Recently, several experimental and theoretical studies on this phenomenon have been made. However, experimental results to date have been limited to polymer solutions.

In the present study, an apparatus has been designed and constructed to study the "Weissenberg effect" in molten polymers. Three commercial polyethylene resins were studied: one high density polyethylene (HDPE) at 190°C, and two low density polyethylenes (LDPE) at 182°C. For each resin, the variation of the height of rise with the angular velocity was determined: for the HDPE, the height varies linearly with the velocity, for one LDPE, the height is proportional to the square of the angular velocity. For the two LDPE resins, curves of height of rise versus time were obtained, and it was observed that at higher speeds, after a fairly rapid increase, the height leveled off for a period of time, then increased again until a second steady state value was reached. The resin which had the highest viscosity and lowest density gave the greatest height of rise.

RÉSUMÉ

Un fait curieux bien connu dans le domaine de Rhéologie expérimentale est la tendance des liquides viscoélastiques de grimper à la surface d'un cylindre tournant dans un grand récipient de liquide. Ce phénomène est communément appelé l'"Effet Weissenberg". Récemment, plusieurs études expérimentales et théoriques sur ce phénomène ont été réalisées. Cependant, les résultats expérimentaux jusqu'à ce jour ont été limités aux solutions de polymère.

Dans la présente étude, un montage expérimental a été conçu et construit pour étudier l'"Effet Weissenberg" dans les polymères fondus. Trois résines commerciales de polyéthylène ont été étudiées: une de haute densité à 190°C et deux de basse densité à 182°C. La variation de la hauteur de montée pour chaque résine a été déterminée en fonction de la vitesse angulaire: il a été observé que, pour le polyéthylène de haute densité, cette hauteur varie linéairement avec la vitesse, tandis que pour un des deux polyéthylènes de basse densité, la hauteur de montée est proportionnelle au carré de la vitesse angulaire. On a reporté les valeurs de la hauteur de montée en fonction du temps et on a observé que pour les grandes vitesses, après une assez rapide augmentation, la hauteur se stabilise pendant un certain temps, puis remonte à nouveau jusqu'à atteindre une seconde valeur stationnaire. La résine qui a la plus grande viscosité et la plus basse densité accuse la plus haute montée.

TABLE OF CONTENTS

	<u>Page</u>
ACKNOWLEDGEMENTS	i
ABSTRACT	ii
RESUME	iii
TABLE OF CONTENTS	iv
LIST OF FIGURES	v
LIST OF TABLES	vi
CHAPTER 1. INTRODUCTION	1
Review of the Previous Work	2
Objectives of the Present Study	9
CHAPTER 2. EXPERIMENTAL EQUIPMENT AND PROCEDURE	10
Description of the Equipment	10
Experimental Procedure	16
CHAPTER 3. EXPERIMENTAL RESULTS AND DISCUSSION	19
Resin 10	19
Resin 1	27
Resin 4	32
Discussion of Results	37
CHAPTER 4. CONCLUSIONS	40
BIBLIOGRAPHY	42
NOMENCLATURE	43

LIST OF FIGURES

<u>Figure</u>		<u>Page</u>
1	Overall View of the Equipment	11
2	The Cylindrical Container	11
3	Side View Drawing of the Equipment	12
4	Diagram of the Electrical Circuit Showing the Connections of the Heaters to the Controller	15
5	Scheme of the Reference Grid	18
6	Viscosity versus Shear Rate Curve for Resin 10	20
7.1-7.8	Evolution of the Free Surface Shape for $\Omega = 1$ rpm	22
8.1-8.3	The Shape of the Free Surface at Various Angular Velocities for Resin 10	23
9	Rise Versus Time Curve for Resin 10	24
10	Rise versus Angular Velocity for Resin 10	25
11	Viscosity versus Shear Rate Curve for Resin 1	29
12.1-12.2	The Change of the Free Surface Shape for Resin 1	28
13.1-13.5	The Shape of the Free Surface at Various Angular Velocities for Resin 1	23
14	Rise Versus Time Curve for Resin 1	31
15	Rise versus Square of the Angular Velocity for Resin 1	33
16	Viscosity versus Shear Rate Curve for Resin 4	34
17.1-17.8	The Shape of the Free Surface at Various Angular Velocities for Resin 4	35
18	Rise versus Angular Velocity Curve for Resin 4	36

LIST OF TABLES

		<u>Page</u>
TABLE I	Experimental Data for Resin 10	21.
TABLE II	Experimental Data for Resin 1	30

CHAPTER 1

INTRODUCTION

When a vertical rod is immersed in a container of inelastic fluid and is rotated, the fluid flows outward until its surface assumes a parabolic profile with the lowest point at the rod. In this state, the radial gradient in the hydrostatic head balances the centripetal acceleration. A viscoelastic fluid, on the other hand, will climb up the rod. This phenomenon has been referred to as "rod-climbing" or the "Weissenberg effect". The shape of the free surface in this case is determined by a balance of centripetal acceleration, normal stresses and gravity. It is the normal stress differences, characteristics of viscoelastic fluids, which are responsible for the climbing effect. Indeed, one may visualise the normal stresses in the direction of flow as an extra tension which arises along the streamlines. In the case of flow between rotating cylinders, these are circles, and the stresses acting on a fluid element in this flow may be represented as below:



The sum of forces along the radius on the fluid element is in the inward direction, so that the fluid is squeezed toward the rod. With fixed boundaries at the rod and the bottom, the fluid must move upward along the shaft until the gravitational head balances this stress.

The phenomenon of "rod-climbing" is of importance in the design of polymer processing equipment and in instruments for rheological measurements, and it has been the object of several theoretical and experimental studies. However, experimental studies to date have been limited to polymer solutions, and no studies of rod-climbing in melts have been reported.

Review of Previous Work

Weissenberg (13) was the first investigator who publicized the climbing phenomenon in viscoelastic fluids, and he postulated that the phenomenon was associated with the existence of normal stress differences, basing this conclusion on a series of demonstrations. His experimental arrangement was such that the liquid was sheared in a gap between an outer vessel rotated with an angular velocity that was kept constant at various levels, and an inner cylinder which was held stationary. An analysis of the experimental results showed that in such a motion, the stress has its strength so distributed over the various directions in space as to comprise, in addition to the shear stress components, a tensile stress along the lines of flow. The presence of such a tensile stress was made conspicuous by stopping the motion, and then making cuts perpendicular to the lines of flow: the tensile component in the stress caused the cuts to open up. When the lines of flow are closed circles, the tensile force along these lines "strangulates" the liquid and forces it inwards balancing not only the centripetal acceleration but also a gravitational head.

A few years later, Garner and Nissan (4) continued the investigation on the normal-stress effects with an experimental study of surface

climbs associated with the Weissenberg effect. A photographic study to determine the cross-sectional profile of the climb was made. The results showed that the shape of the climb followed an "inverse-fourth-power" relationship, of the form $h = Ar^{-4}$, where A was a constant, if points near the two wall boundaries were neglected.

This result was in good agreement with the theoretical result obtained by Oldroyd (10), who based his calculations on a non-linear, eight-constant rate model and made use of the steady Couette velocity profile for a Newtonian fluid in his analysis, although we now know that this is unrealistic when dealing with viscoelastic fluids.

The secondary flow associated with the Weissenberg effect was first observed by Saville and Thompson (11) in an interesting experiment. They suspended a viscoelastic fluid in a layer with immiscible Newtonian fluids above and below between concentric vertical cylinders. When the inner cylinder was rotated, a double Weissenberg effect was observed, with the viscoelastic fluid both rising and extending downward at the inner cylinder. Dye was used as a tracer to show the streamlines of the secondary flow. There is still doubt whether the secondary motion here is a result of perturbation due to a surface effect rather than a characteristic of the Weissenberg effect.

To explain the phenomenon of rod-climbing, Chezeaux (3) developed a constitutive equation which could describe properly the behaviour of the fluids exhibiting this phenomenon by combining the theory of Rivlin for non-linear purely viscous fluid and a theory which introduced the

effect of elasticity. Using this equation, she calculated the shape of the free-surface of the climbing fluid. A good agreement was obtained at low speeds between the theoretical and experimental results for polyisobutylene and polystyrene solutions.

Chan (2), in an attempt to arrive at a detailed explanation of the actual mechanism involved in the climbing phenomenon, has considered together the experimental and theoretical aspects of the effect. The free-surface shape of the climbing and the velocity profile were determined experimentally by an optical technique for several polymer solutions. The results showed that the tangential velocity profiles had a completely different character from the more commonly known one for a Newtonian fluid, and the "inverse-fourth-power-of-radius" suggested by previous investigators was not obeyed. He did not observe any secondary flow. In his theoretical work, Chan carried out a numerical simulation of the Weissenberg effect. The Rivlin-Erickson fluid model for viscometric flow was used to describe the behaviour of the fluid, and the problem was solved by a finite-difference method. The comparison of experimental data with theoretical results showed only qualitative agreement. Furthermore, theoretical results indicated the existence of radial and axial velocity fields, whose values were extremely small, and negligible within the limits of experimental accuracy. This result left the question of the existence of the secondary flow unresolved.

Hoffman and Gottenberg (5) developed a theory which directly related the climbing phenomenon to the viscometric functions of a simple fluid. By applying the free-surface shape boundary conditions to equations

of motion, they were able to develop a relationship between the two normal stress differences and the quantities on the free-surface which might be measured experimentally, such as the free-surface profile and surface velocity profile. In their calculations, they neglected surface tension effects and the secondary flow. A good comparison was obtained between the material functions determined from their theory and those published previously for isobutylene solutions. Hoffman and Gottenberg also pointed out that the second normal stress difference was a very small quantity and that the secondary flow observed experimentally was negligible.

By using a perturbation procedure, Kaye (8) was able to calculate the shape of the free surface of climbing for a "fluid of grade 2" whose constitutive equation takes the form:

$$p_{ij} + p\delta_{ij} = \nu\rho A_{ij}^{(1)} + \alpha_2\rho A_{ik}^{(1)}A_{kj}^{(1)} + \alpha_1\rho A_{ij}^{(2)}$$

where p_{ij} are the components of the stress tensor referred to a set of rectangular Cartesian co-ordinate axes, p is the magnitude of the isotropic pressure, ν , α_1 , α_2 are constants and ρ is the density of the liquid. $A_{ij}^{(1)}$ is defined by

$$A_{ij}^{(1)} = \frac{\partial v_i}{\partial x_j} + \frac{\partial v_j}{\partial x_i}$$

where v_i is the velocity of a typical particle of the liquid, and

$$A_{ij}^{(2)} = \frac{\partial A_{ij}^{(1)}}{\partial t} + v_k \frac{\partial A_{ij}^{(1)}}{\partial x_k} + A_{ik}^{(1)} \frac{\partial v_k}{\partial x_j} + A_{kj}^{(1)} \frac{\partial v_k}{\partial x_i}$$

ϕ_{ij} has its usual meaning and the dummy suffix notation is employed. The result showed that the climbing only occurred when $3\alpha_1 + 2\alpha_2$ was positive. The shapes of the climbing surface observed experimentally for some polymer solutions did not conform to the prediction of the theory. However, an interesting conclusion was drawn from the study of Kaye: if there was agreement between theory and experiment, the theory would give an indirect method of measuring normal stress differences, at very much lower levels than those measured previously.

The most elaborate work on rod-climbing was done by Joseph and Fosdick (7). They used the method of perturbation about the state of rest, which was constructed as a series in powers of Ω , the angular velocity of the rotating rod, to calculate the profile of the free surface of the rotating fluid. In their work, they considered first the case of a Newtonian fluid, and carried their calculations as far as terms of the fourth order in Ω . At zeroth order, there was a flat surface with atmospheric pressure above and hydrostatic pressure below. At order Ω , a velocity field appeared without change of pressure. There was no deviation from a flat surface at this order. At order Ω^2 , there was no velocity gradient correction, but a pressure change was induced. At order Ω^4 , a secondary motion appeared: the fluid began to circulate up and down along the axial direction, and in and out along the radial lines. After that, Joseph and Fosdick turned their attention to simple fluids. By use of the retardation theorem of Coleman and Noll, they could resort to the explicit constitutive relation of the fluid of grade n , and they carried

their calculation as far as grade 4. Through the fourth order in Ω , they found that the shape of the free-surface depended solely on constants which are related to the three viscometric functions. At order four, as in the case of Newtonian fluids, secondary motions first appeared.

After that, Joseph, Beavers and Fosdick (6) turned their attention to the "fluid of grade two". The same results as those obtained by Kaye were found: at second order of Ω , the shape of the free surface was determined by $3\alpha_1 + 2\alpha_2$, and when this coefficient is positive, the fluid climbs the rod. But Joseph, Beavers and Fosdick went further. They calculated the shape of the free surface for two cases. In the first case, the effects of surface tension were neglected, and in the second case, these effects were considered. The results obtained for both cases were then tested by a series of experiments. The experimental apparatus used consisted mainly of a rod of uniform diameter rotating at constant angular velocity in a vat completely filled with "STP" motor oil additive. Rods of several diameters were used, and for each rod, photographs of the surface profiles were taken for various values of the angular velocity. The following results were obtained:

-For small values of Ω ($\Omega^2 < \frac{12}{a^{1/2}}$, where Ω is the number of revolutions per second, and a the radius of the rod), the rise of the free surface at the rod was proportional to Ω^2 , as predicted by the theory, and its shape was concave.

-For larger values of Ω , i.e. $\Omega^2 \approx \frac{12}{a^{1/2}}$, the rise at the rod increased less rapidly, and the free surface assumed a convex shape.

-At even larger values of Ω , the steady configuration lost its stability to motion periodic in time. A band of fluid seemed to rise

slowly almost to the full-height of the raised column of fluid and then to collapse downwards to the surface of the main body of the fluid.

-STP motor oil additive climbed up a small rod but not a large one. This fact was predicted by the theory.

-The observed shapes of the free-surface did not conform to the prediction of the theory devoid of surface tension. But they were in striking agreement with the theoretical profiles, when the surface tension was considered, for small values of $\Omega (\Omega^2 < \frac{12}{a^{1/2}})$. This agreement left open the possibility that an accurate determination of the form of the free-surface would yield information about the viscometric functions.

Beavers and Joseph (1) continued their work on rod climbing, and in their most recent paper, more results were reported. In their previous experimental work with STP oil, they observed some climb due to wetting when $\Omega = 0$, so that a static rise, determined from experimental data, should be added to the rise computed from theory to give a good agreement. By coating the rod with "Scotchgard", this problem of static rise was eliminated, and an excellent agreement between the theoretical shape and the experimental shape was obtained. The condition that a flat contact with the rod as the fluid climbed up the rod must be maintained, assumed in the analysis, was satisfied. The curve of height versus Ω^2 was always a straight line, and had the same slope as the one obtained before, when the rod was uncoated. The effect of temperature on the parameter $3\alpha_1 + 2\alpha_2$ (called $\hat{\beta}$ in the paper) was investigated. It was found that the value of $\hat{\beta}$ was very sensitive to changes in temperature. As the temperature is increased, a large decrease was expected in the value of $\hat{\beta}$. For a higher temperature studied, as the rotational speed

was increased to very high values, the rise decreased and was replaced with an inertia-dominated depression of the free-surface. For a rod of given radius, when the fluid temperature was raised, the climb on the rod at all rotational speeds was completely eliminated. This phenomenon was predicted by the theory. Another fluid, a solution of polyacrylamide in glycerine water mixture, was used to test the second-order theory. It was found that the second-order theory could be applied for this solution, provided the temperature was such that there was a discernable range of rotational speeds for which $h(a, \Omega^2)$ was linearly proportional to Ω^2 . Joseph and Beavers also mentioned in this paper that there was a range of rotational speeds for which STP oil might have been well described by the "fluid of grade 4".

Objectives of the Present Study

The review of the literature on rod-climbing shows that several experimental and theoretical studies have been made. However, in each case, the fluids studied were polymer solutions. No studies of rod-climbing in polymer melts have been reported. The object of the present study is to demonstrate "rod-climbing" in melts and to make measurements of the free surface shape for several polymers. It is hoped that this work will lead ultimately to the development of a simple experimental test for characterizing commercial thermoplastic resins.

CHAPTER 2

EXPERIMENTAL EQUIPMENT AND PROCEDURE

The study of rod-climbing in polymer melts requires the design and construction of a special apparatus. The basic problem is to provide simultaneously for good temperature control and good visibility of the free-surface, and to minimize the degradation of the melt.

In this chapter, descriptions of the equipment and the experimental procedure are given.

Description of the Equipment

An overall view of the equipment is shown in Fig.1. It consists mainly of an insulated box mounted on a platform. A stand, which is used simultaneously as a support for a temperature controller and a motor-generator is fixed to the platform. The motor-generator is connected to a speed controller. The insulated box has three windows of Pyrex glass, one for taking photographs, the other two for lighting. The position of the camera, and the technique of lighting are shown in Fig.1. Inside the box are eight heaters and a central vertical rod. A scheme of the box and its contents is given in Fig.3. The heaters are connected to the temperature controller mentioned above. The rod goes through a hole in the cover of the box at its center, and is connected to the motor-generator by a coupling. The cylindrical container consists of two parts, a Pyrex tube and a stainless steel plate used as the base for the container. A photograph of it is shown in Fig.2. This plate is provided with four vertical rods at its four corners. These rods go through four openings



FIGURE 1. Overall View of the Equipment .

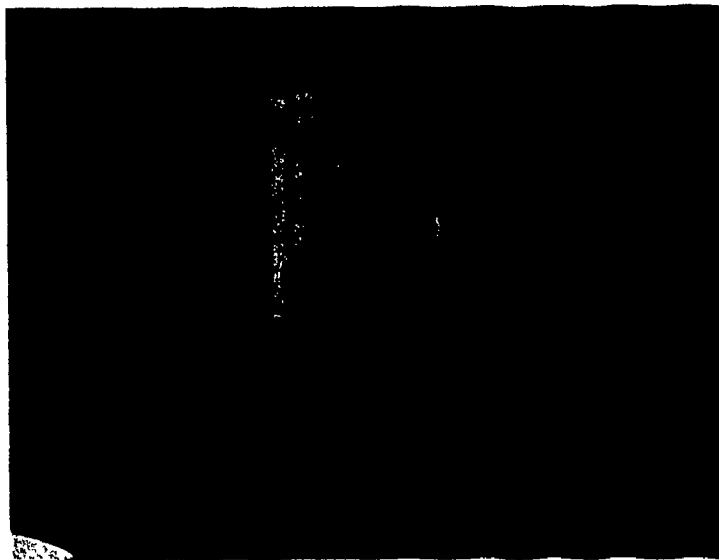
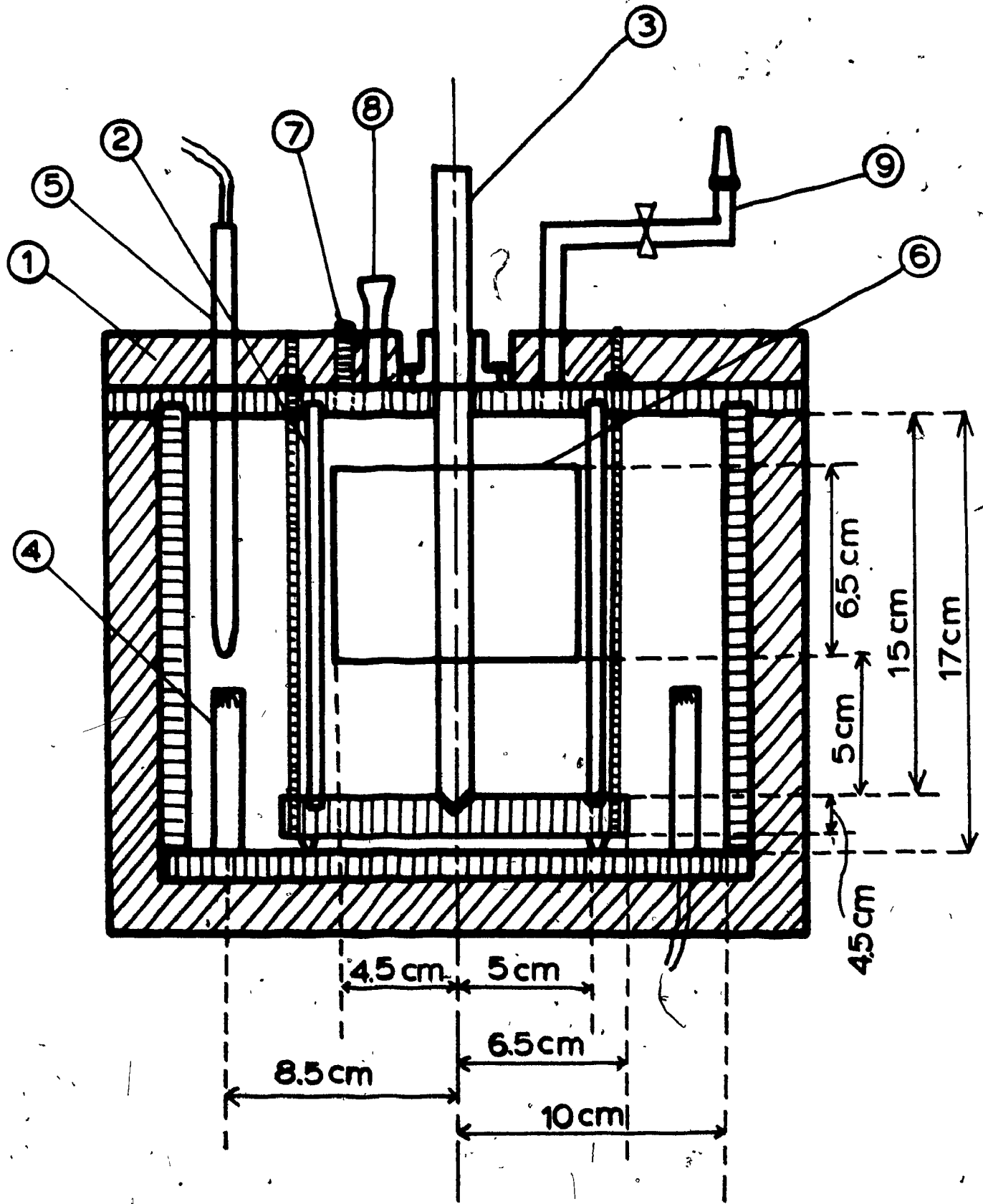


FIGURE 2. The Cylindrical Container

FIGURE 3. Side View Drawing of the Equipment

1. cover of the insulated box
2. pyrex tube
3. rotating rod
4. heaters (8)
5. thermocouple
6. window (3)
7. inlet for the nitrogen
8. check valve
9. system for making the vacuum
fiberglass
stainless steel



bored in the cover, and four bolts are used to hold the container and the cover strongly together. In this way, the positions of the container and the rod are fixed, with respect to each other, and with respect to the cover. Besides the openings for the rotating rod, and the four rods of the container, the cover has other openings: the first one is for the thermocouple lead wires, which are connected to the temperature controller, the second one for the inlet of the nitrogen, the third one for a check valve, and the last one is used for drawing a vacuum inside the container. The vacuum system consists of a copper tube and a shut-off valve connected to a vacuum pump by means of a plastic tube, as shown in Fig.1.

The principal dimensions are given in Fig.3. The purpose of drawing a vacuum is to eliminate the inclusion of bubbles in the melt and to remove all the oxygen present in the container. After evacuation and melting, dry nitrogen is introduced; it constitutes an inert medium inside the polymer container, thus avoiding the oxidation of the melt. It is supplied from a cylinder fitted with a regulator and a check valve.

The outer box is made with stainless steel plates of .5 centimeters in thickness, welded together. It is insulated by fiberglass, and the insulation thickness is 2.5 centimeters. This box is used as a heating system to melt the polymer, and also as a medium for temperature control.

An on-off proportional controller, Model 32106, purchased from Thermo Electric Co., is used with an Iron Constantan thermocouple furnished by the same company.

The heaters used are cartridge heaters. Four of them have 475 watts each, and the other four 120 watts each, giving a total of 2380 watts. This total exceeds the limit which can be operated by the controller, so that a relay is needed. The heaters are connected in parallel and are related to the controller as shown in Fig.4.

On the base plate of the container, there is a circular groove containing a viton O-ring. The purpose of this groove is to keep the Pyrex cylinder in place and to prevent air contamination when there is a vacuum inside the container or the leakage of nitrogen when nitrogen is inside. There is a similar groove in the cover, for the same purpose.

The rotating rod is 12.5 mm in diameter, and 18 cm long. It is made of stainless steel. The end of the rod, having a conical shape, goes into a conical hole made at the center of the circular groove mentioned above. This is to make sure that the rod is properly centered.

The motor generator and the speed controller were purchased from Cole-Parmer Instrument Company (Model E650-MG, and Model 20-1, respectively). The controller furnishes a visual indication of the motor speed. The motor shaft has two ends: direct drive is obtained at one end, and the value indicated is the true speed; at the other end (the geared end), speed reduction is obtained; the value indicated must be divided by the gear reduction ratio to give the true speed. In this research, the gear reduction ratio was 20:1, and the geared end was used. This permitted studies at very low speeds.

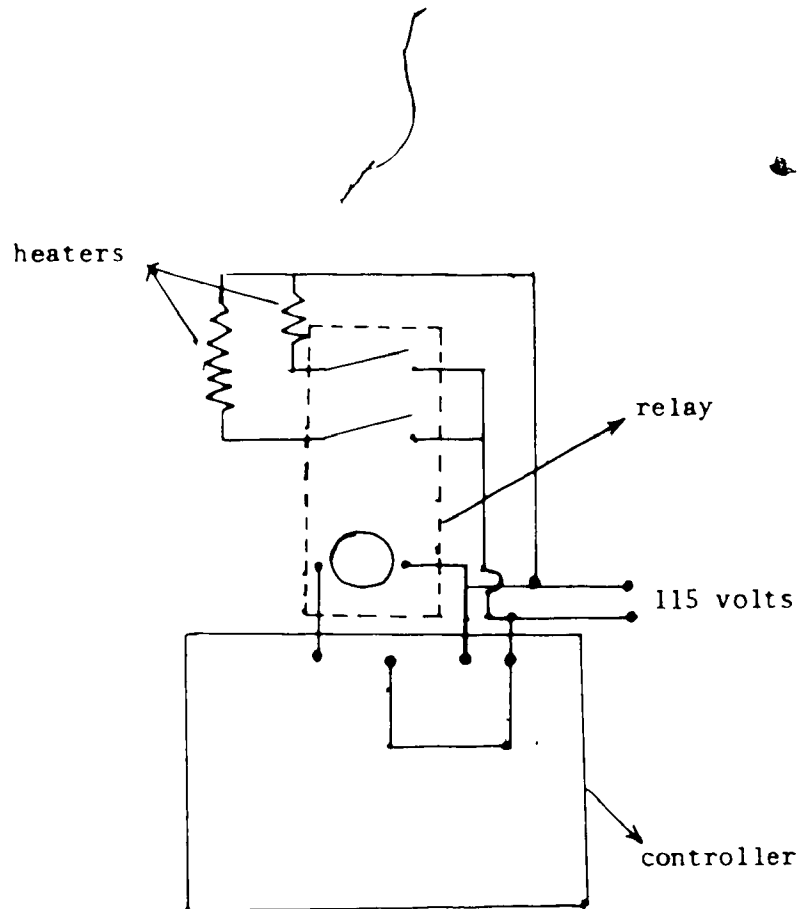


FIGURE 4. Diagram of the Electrical Circuit Showing the Connections of the Heaters to the Controller

Experimental Procedure

1. The coupling which connected the rod and the motor shaft is made of two parts so that the motor can be easily uncoupled from the shaft for assembly and disassembly of the apparatus.

2. The cover, the rod and the container, which form a single unit, are removed together from the outer box.

3. By unscrewing the nuts which hold these parts together, we can separate them.

4. The polymer, in granular form, is poured into the container, up to a height of 6 centimeters.

5. The cover is placed over the container, the four rods of the container going through the four rod holes of the cover. Four nuts are used to hold the container and the cover firmly together.

6. The hole for the passage of the rod is sealed by a piece of metal.

7. The valve of the vacuum system is closed. Nitrogen is introduced into the container. Any leakages are detected by a leak detector. These leakages can be eliminated by adjusting the nuts which hold the different parts together. When all leakages are eliminated, the container and the cover are placed in the insulated box. The nitrogen cylinder is closed, the shut-off valve is opened, and the vacuum pump is turned on. The temperature controller is plugged in.

8. The polymer melts most rapidly at the bottom. When half of the polymer is melted (this takes about one hour), the nitrogen cylinder is opened, the vacuum system valve closed, and the vacuum pump turned off. After one more hour, the polymer is completely melted. The piece of metal used to seal the hole is removed, and the rod is introduced. One part

of the coupling is fixed to the shaft of the motor, the other part goes with the rod.

9. The insulated box is placed under the motor so that the rod is exactly under the shaft of the motor, and the two parts of the coupling can be connected.

10. If the surface of the melt is not completely flat it is necessary to wait a few minutes until it becomes flat. One can now start the motor, and set the speed at the desired value.

11. For one speed, photographs of the surface profile are taken at brief intervals, until the steady state is reached. This may take from 3 to 5 hours.

12. When data have been obtained for one speed, the nitrogen supply is shut-off, the temperature controller disconnected and the speed controller is turned off. Steps 1, 2, and 3 are repeated. The Pyrex tube and the plate are separated. The polymer melt is removed as much as possible from the rod, the glass tube and the plate. Tetrahydronaphtalene is used to remove the remaining parts of the melt.

13. When everything is cleaned, steps 4 to 12 are repeated and another set of data is obtained.

The distance from the place where the rod-climbing phenomenon occurs to the camera is kept constant, so that the distances can be determined by use of a photograph of a reference grid. This reference grid is illustrated in Fig.5.

This grid is inserted in place of the rod, and a photograph of it is taken so that the distance from it to the camera is the same as the distance from the "climbing" profile to the camera.

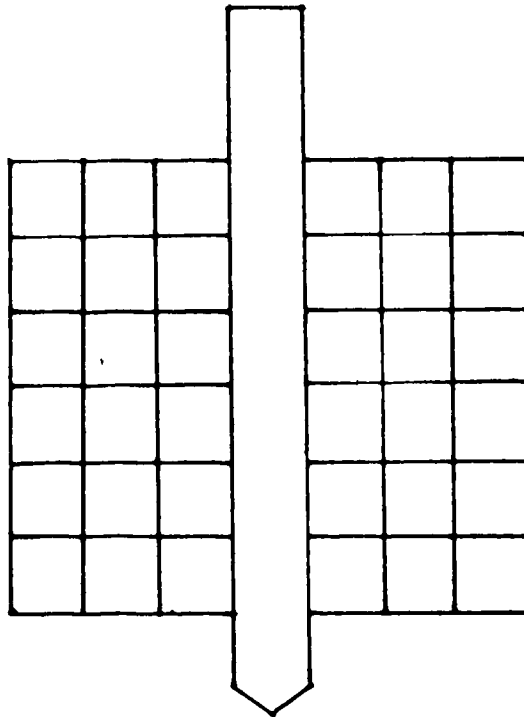


FIGURE 5. Scheme of the Reference Grid

CHAPTER 3

EXPERIMENTAL RESULTS AND DISCUSSIONS

Three different types of polyethylene resin were studied in this work. For convenience, these will be referred to by use of their inventory numbers in the McGill Polymer Engineering Laboratories.

Some characteristics and the experimental results obtained for these resins are given in this chapter.

Resin 10

This resin has the following characteristics:

- low density polyethylene
- unmodified film-resin DFDQ 4400
- made by Union Carbide of Canada Ltd.
- highly branched - low molecular weight
- density: .915 g/cc

The data on viscosity are given in Fig.6.

The experimental results obtained for this resin are given in Table I, in Figs. 7.1 through 7.8, in Figs.8.1 through 8.3, and in Figs. 9 and 10.

All the experiments were performed at 182°C, and under a slightly positive pressure of nitrogen to eliminate air (in this research, we take 1 psig).

FIGURE 6. Viscosity versus Shear Rate Curve for Resin 10

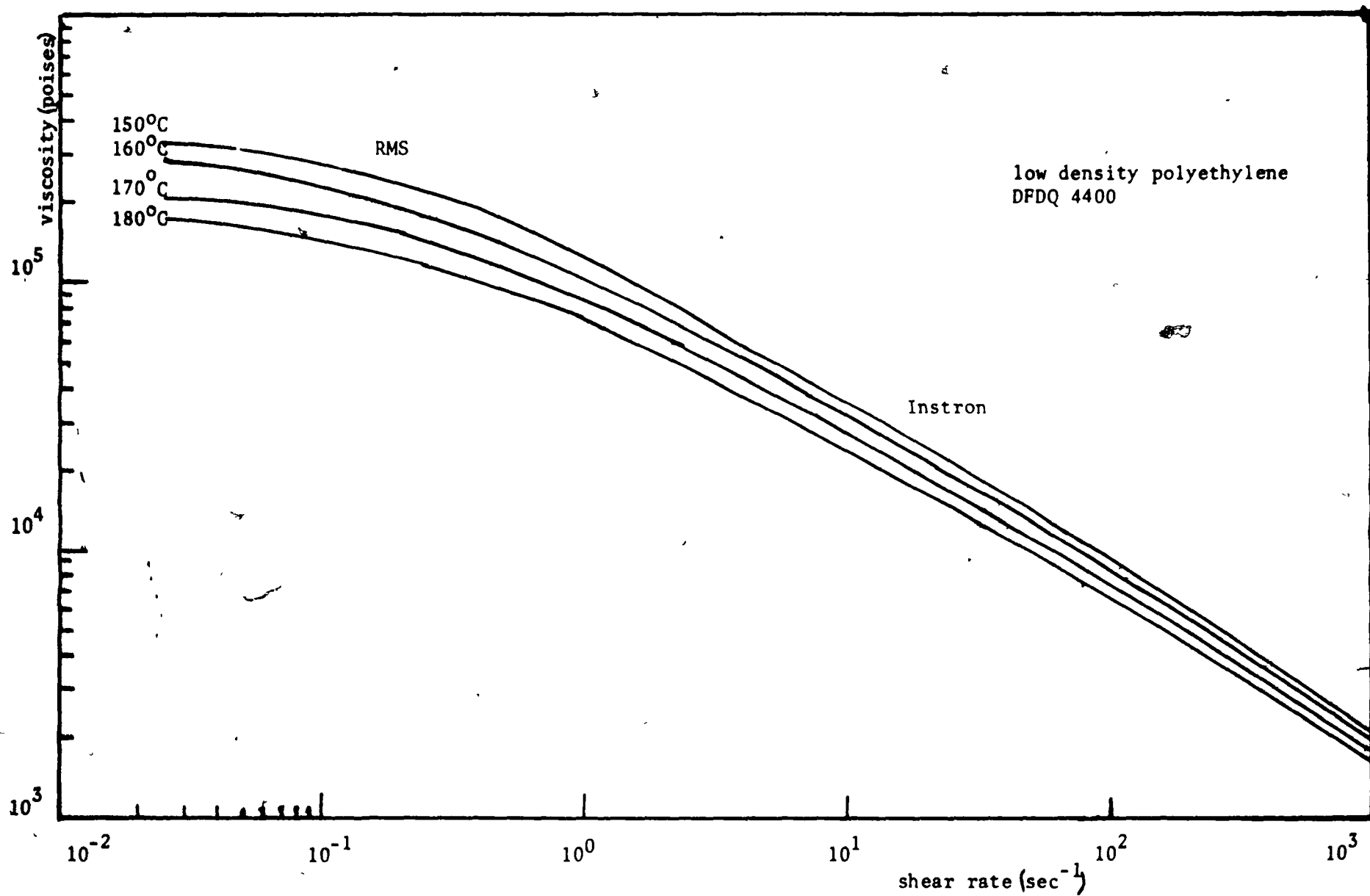


FIGURE 6

TABLE I

Experimental Data for Resin 10

Ω - .25 rpm

t(min)	20	50	90	130
h(cm)	.27	.36	.50	.55

Ω - .50 rpm

t(min)	10	15	20	30	40	55	105	170
h(cm)	.84	.98	1.11	1.25	1.26	1.31	1.40	1.45

Ω - .75 rpm

t(min)	6.5	15	24	30	41	50	57	60
h(cm)	.87	1.47	1.78	1.87	1.91	2.	2.	2.

t(min)	65	78	85	92	106	125	142	152
h(cm)	2	2.4	3.09	3.18	3.39	3.56	3.6	3.65

Ω - 1 rpm

t(min)	2	4	6	11	15	21	32	36
h(cm)	.54	.91	1.58	1.95	2.23	2.43	2.43	2.43

t(min)	55	70	90	100	130	145	155	165
h(cm)	2.43	2.59	3.32	3.60	4.05	4.15	4.25	4.35

Ω - 1.25 rpm

t(min)	2.5	5	15	24	27	34	42	60
h(cm)	.91	1.6	2.5	2.7	2.72	2.72	2.72	3.

t(min)	80	106	112	129	154	180	240
h(cm)	3.41	3.93	4.03	4.38	4.61	4.8	5.16

t(min)	280	300
h(cm)	5.15	5.16

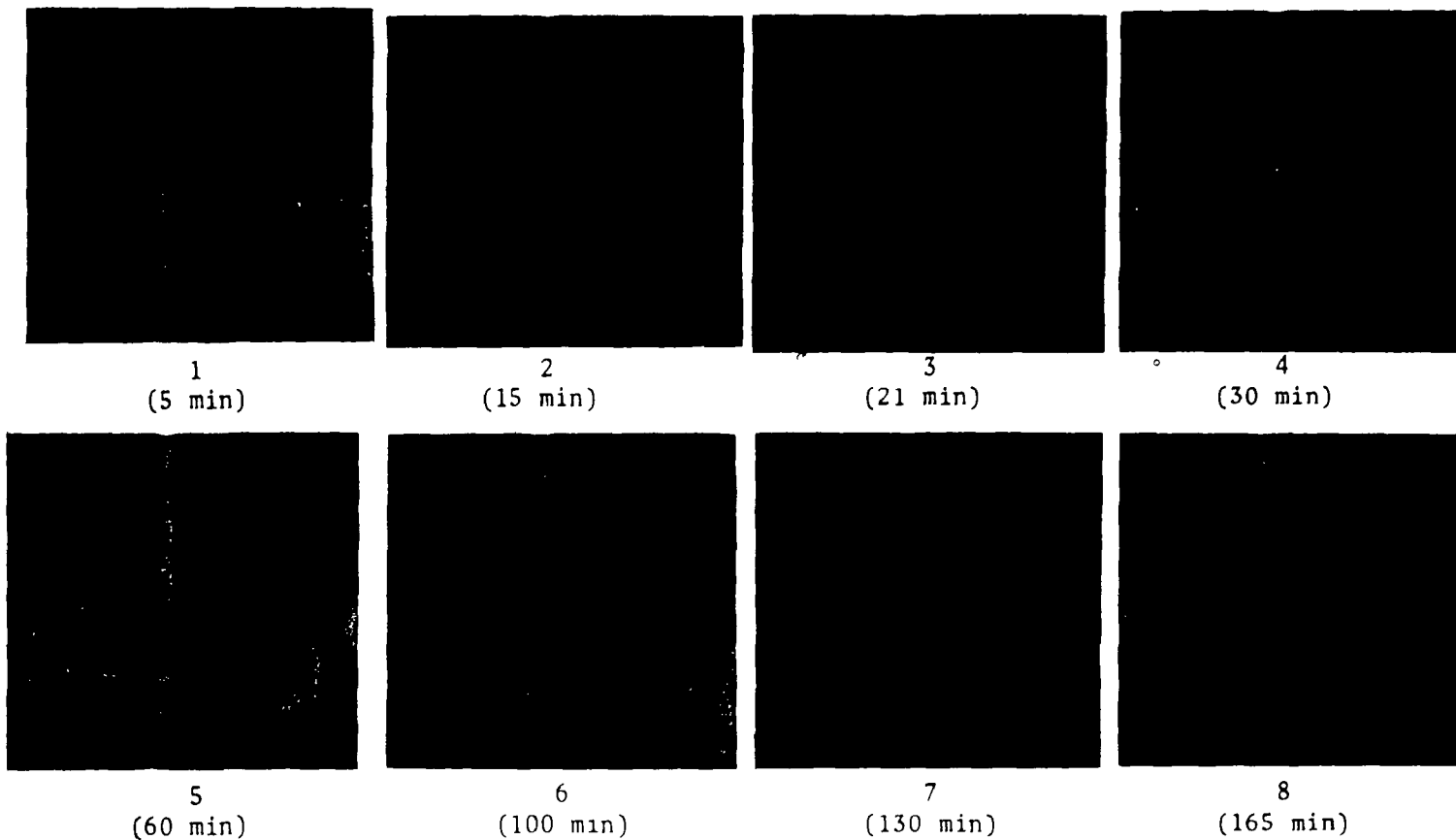


FIGURE 7. Evolution of the Free-Surface Shape for $\Omega = 1$ rpm



1

2

3

FIGURE 8. The Shape of the Free Surface at Various Angular Velocities for Resin 10 ($\Omega = .5, .75, 1.25$ rpm, respectively)



4

5

FIGURE 13. The Shape of the Free Surface at Various Angular Velocities for Resin 1 ($\Omega = .5, .75, 1., 1.25, 2.5$, respectively)

FIGURE 9. Rise versus Time Curve for Resin 10

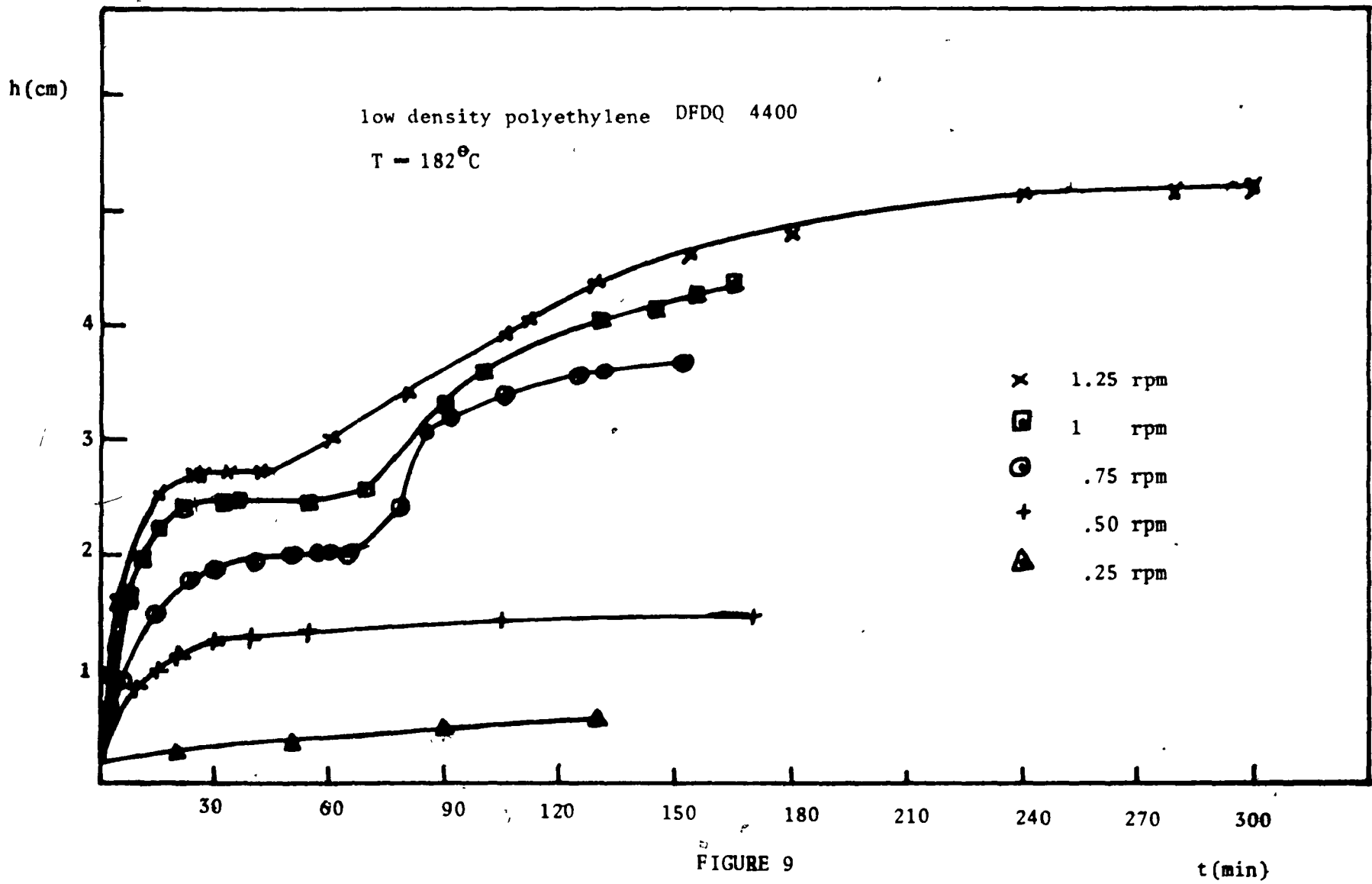


FIGURE 9

FIGURE 10. Rise versus Angular Velocity for Resin 10

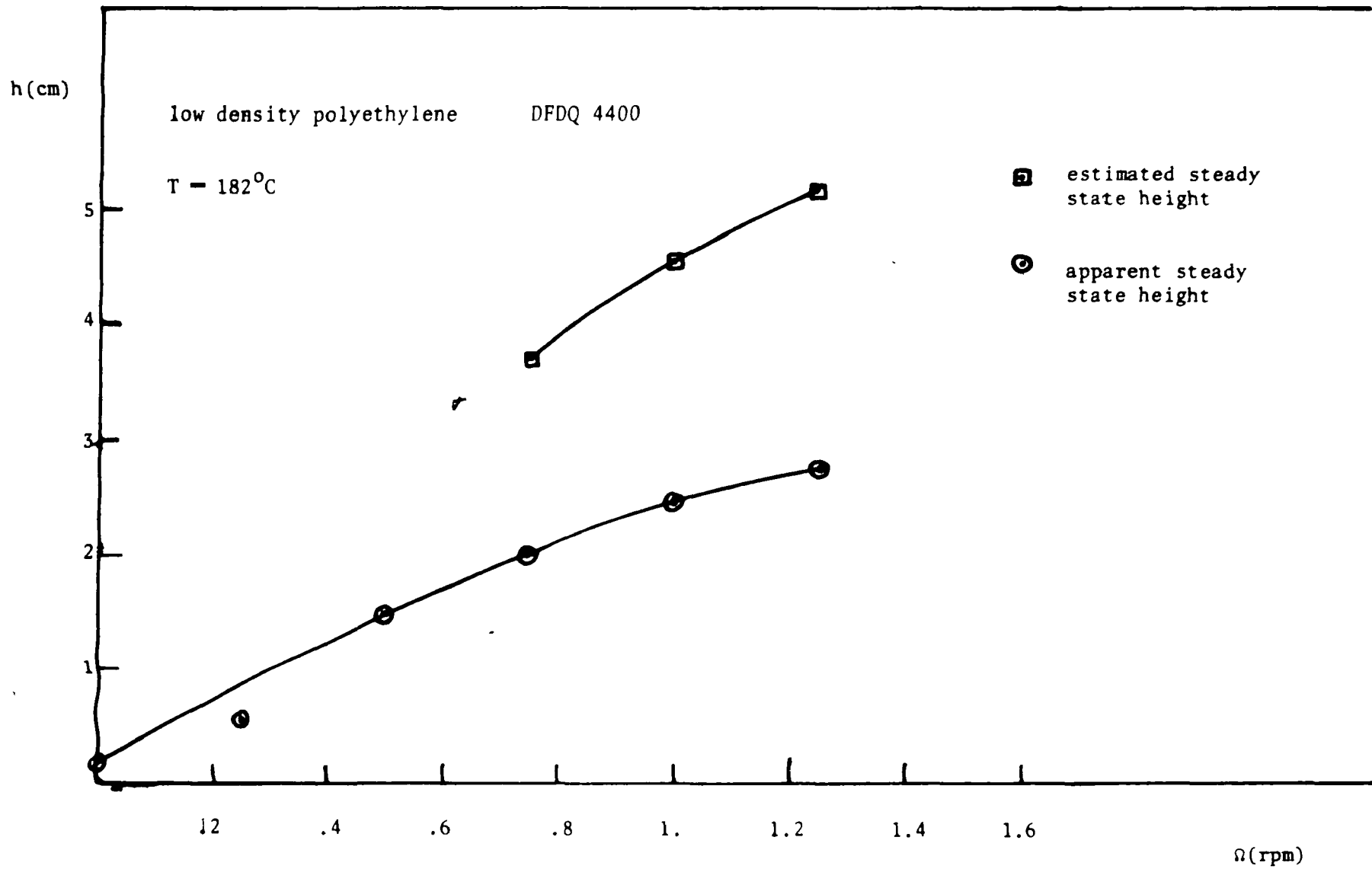


FIGURE 10

Figure 9 shows the graphs of the height rise versus time for five speeds: .25, .50, .75, 1., 1.25 rpm.

For the two lower speeds, the polymer melt rises rather rapidly at the beginning, and the steady state is attained over a period of about two hours.

For the three higher speeds, a bifurcation is observed at the beginning, the polymer climbs up the rod very rapidly, then the speed of rising decreases until it becomes zero: the height keeps a constant value during a period of time varying from 30 to 45 minutes. After this period, the height increases again to attain finally a new steady state.

The photographs of Figs. 7.1 through 7.8 show the evolution of the free surface shape with time for $\Omega = 1$ rpm. Figure 7.1 and Fig. 7.2 give the shape of the climbing surface at 5 and 15 minutes, respectively. During the interval of time from 0 to 15 minutes the height increases very rapidly. At 15 minutes the base of the raised column of liquid begins to contract (Fig. 7.2). From this moment, the rise is less rapid. After 21 minutes (Fig. 7.3), the height reaches a steady value, which is maintained for 30 minutes. During this period, the shape of the free surface changes considerably. The polymer still climbs up the rod, but instead of contributing to the increase of the height, it contributes to the enlarging of the width (Fig. 7.4). After this, the fluid at the top of the raised column starts flowing down, and finally we observe the shape shown in Fig. 7.5. Then, the height increases again rather rapidly (Fig. 7.6). The increase becomes less and less rapid: the polymer which

O climbs up the rod serves simultaneously to increase the height and to enlarge the raised column (Fig. 7.7), and finally, the steady state is attained (Fig. 7.8). During the climbing, the shape of the free surface is not always symmetric: it is alternatively symmetric and assymmetric.

For the two higher speeds, .75 and 1.25 rpm, the shape of the free surface evolves in a similar way.

The shapes of the free surface at steady state for the angular velocity of .5, .75, 1.25 rpm, are shown in Figs. 8.1, 8.2, and 8.3, respectively.

The graphs of the steady height rise versus time and of the apparent steady height versus time are shown in Fig. 120. We note that at $\Omega = 0$, there is some climbing due to wetting. The height increases with the angular velocity Ω , but is not proportional to it, nor to its square.

Resin 1

Some characteristics of this resin are:

- low density polyethylene
- film-grade "Sclair" resin 15-1fE
- made by Dupont of Canada Ltd.
- narrow molecular weight distribution
- density: .921 g/cc

The data on viscosity are shown in Fig. 11.

The experimental results are summarized in Table II, in Figs. 12.1, 12.2, 13.1 through 13.5, 14 and 15.

All the experiments were performed at 182°C and under a pressure of 1 psig.

The graphs of Fig. 14 show the variation of the height rise with time for five angular velocities (.5, .75, 1., 1.25, and 2.5 rpm). For each speed, the height increases rapidly at the beginning, then levels off for a time, and after that it goes on increasing less and less rapidly until the final steady state is attained. These steps are more easily observed at higher speeds.

For the four lower speeds, after the climb height has reached a steady value, the shape of the surface changes from the configuration shown in Fig. 12.1 to the one shown in Fig. 12.2.

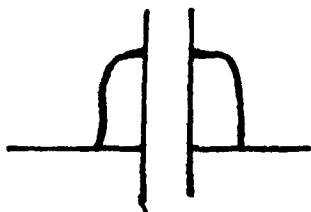


Fig. 12-1

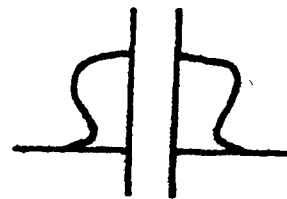


Fig. 12.2

FIGURE 12. The Change of the Free Surface Shape

After that, the height increases again, and the shapes of the surface at steady state assume the forms shown in the photographs of Figs. 13.1 through 13.4 (see p.23), for the angular velocities of .50, .75, 1, and

FIGURE 11. Viscosity versus Shear Rate Curve for Resin 1

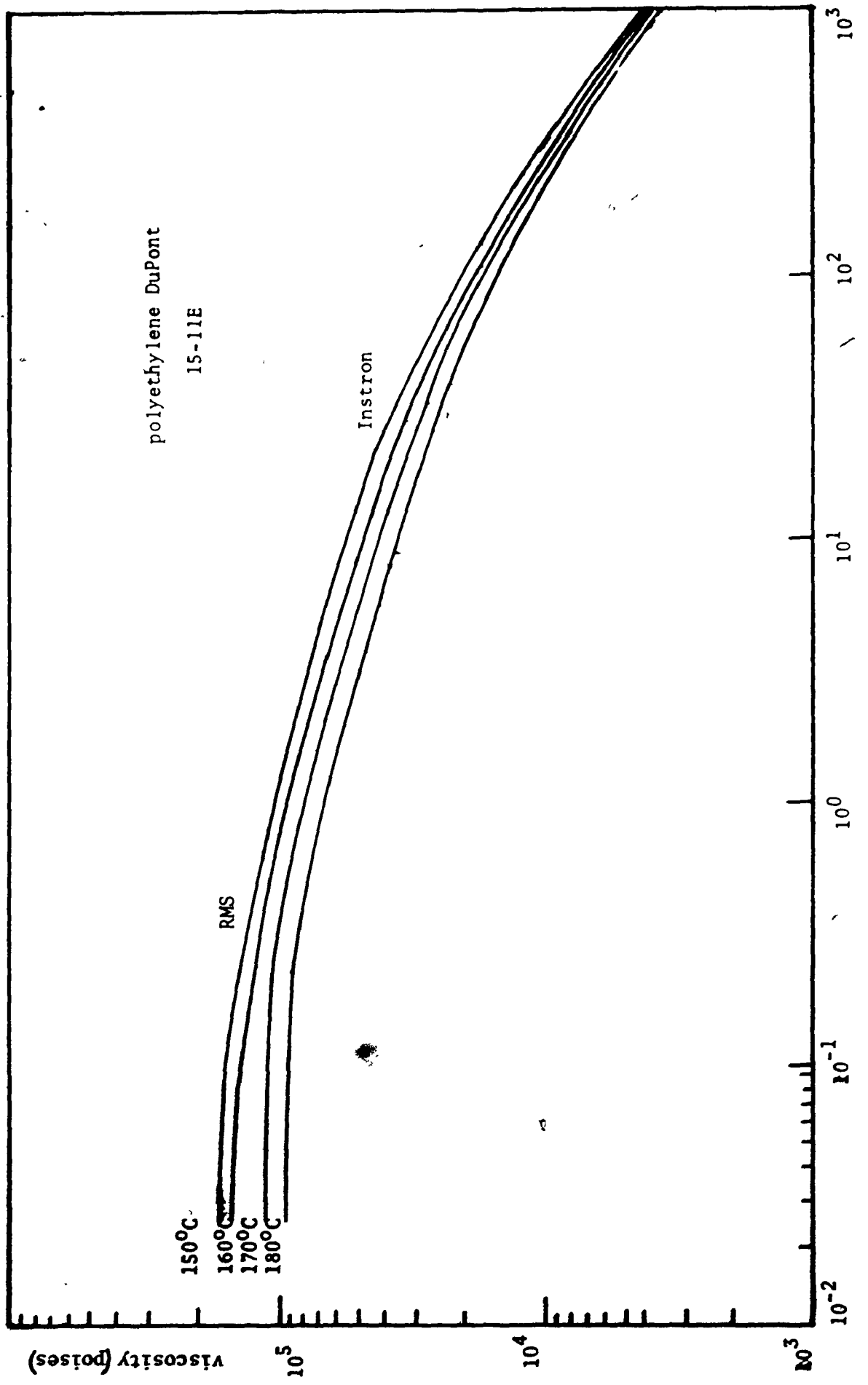


FIGURE 11

TABLE II

Experimental Data for Resin 1

$\Omega = .5$ rpm

t (min)	20	50	73	90	120
h (cm)	.6	.7	.72	.75	.75

$\Omega = .75$ rpm

t (min)	4	10	21	35	75	115	180	240
h (cm)	.4	.65	.92	1.	1.	1.18	1.2	1.2

$\Omega = 1$ rpm

t (min)	5	15	30	45	60	90	120	176	240
h (cm)	.5	.9	1.35	1.5	1.6	1.6	1.77	1.8	1.8

$\Omega = 1.25$ rpm

t (min)	5	10	14	24	28	52	75	90
h (cm)	.7	1.25	1.6	1.9	1.95	2.	2.15	2.25

t (min)	105	130	165	230	270
h (cm)	2.3	2.35	2.50	2.55	2.55

$\Omega = 2.50$ rpm

t (min)	5	11	20	30	34	43	60	76
h (cm)	1.3	2.35	2.75	2.75	2.85	3.1	3.4	3.5

t (min)	120	150	180	210
h (cm)	3.75	3.8	3.8	3.8

FIGURE 14. Rise versus Time Curve for Resin 1

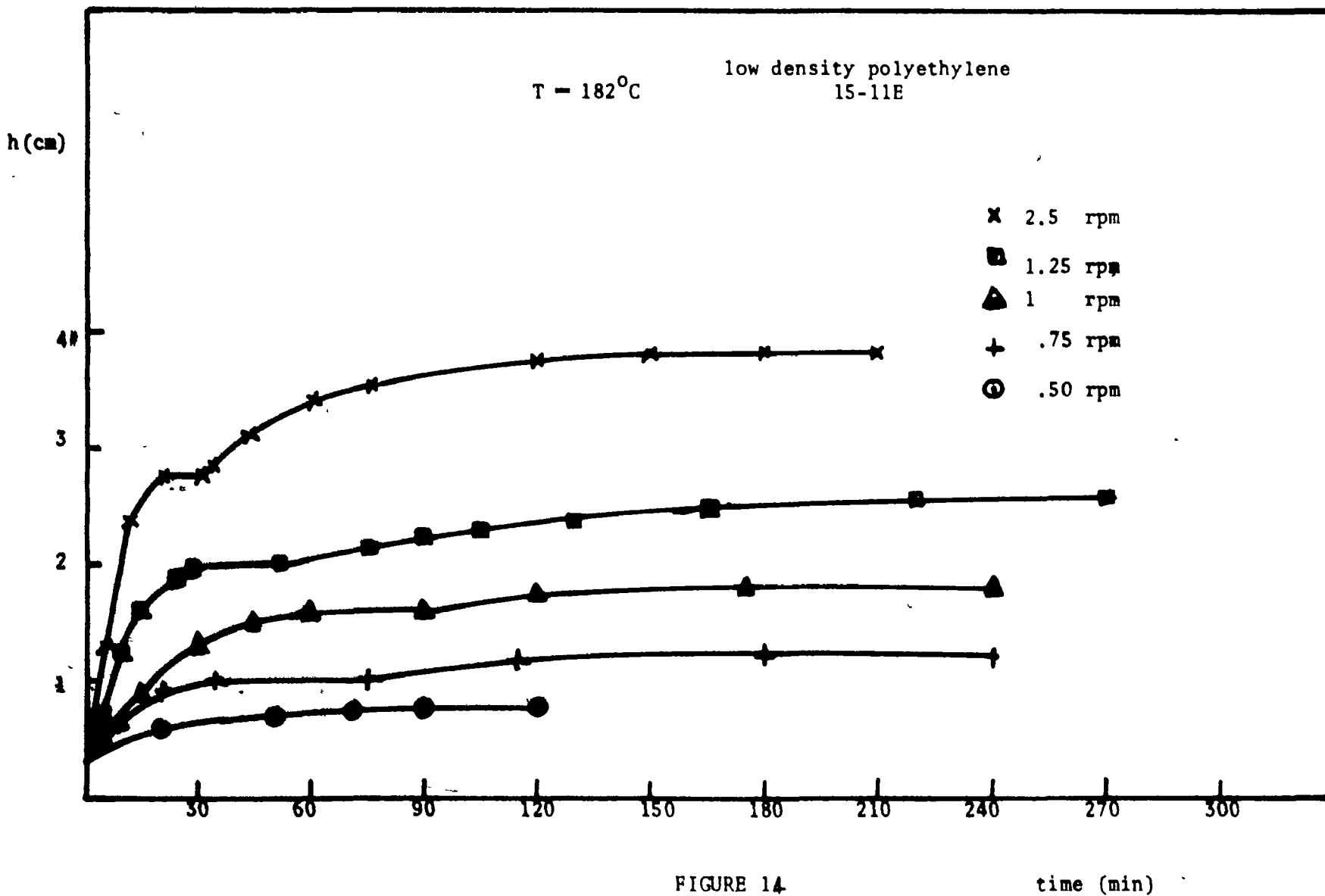


FIGURE 14

time (min)

1.25 rpm, respectively.

For the highest speed studied (2.5 rpm), we observe all the phenomena observed for the higher speeds in resin 10. The shape of the surface at steady state is shown in Fig. 13.5 (p.23).

Figure 15 is a graph of the estimated steady state height versus the square of the angular velocity. This is a straight line, and this is in agreement with the theoretical work obtained by Kaye (8) and by Joseph (6). We also observe some climbing due to wetting when $\Omega = 0$.

Resin 4

This resin has the following characteristics:

- high density polyethylene
- injection-molding "Sclair" resin 2911
- made by Dupont of Canada Ltd.
- molecular weight: 4.8×10^4
- density: .96 g/cm³
- melt index: 25.0

Some data on viscosity are shown in Fig. 16.

All the experiments were performed at 190^o C and under a pressure of 1 psig. The experimental results are summarized in the photographs of Figs. 17.1 through 17.8 and in Fig. 18. For this resin, the steady state is reached very rapidly.

FIGURE 15. Rise versus Square of the Angular Velocity for Resin 1

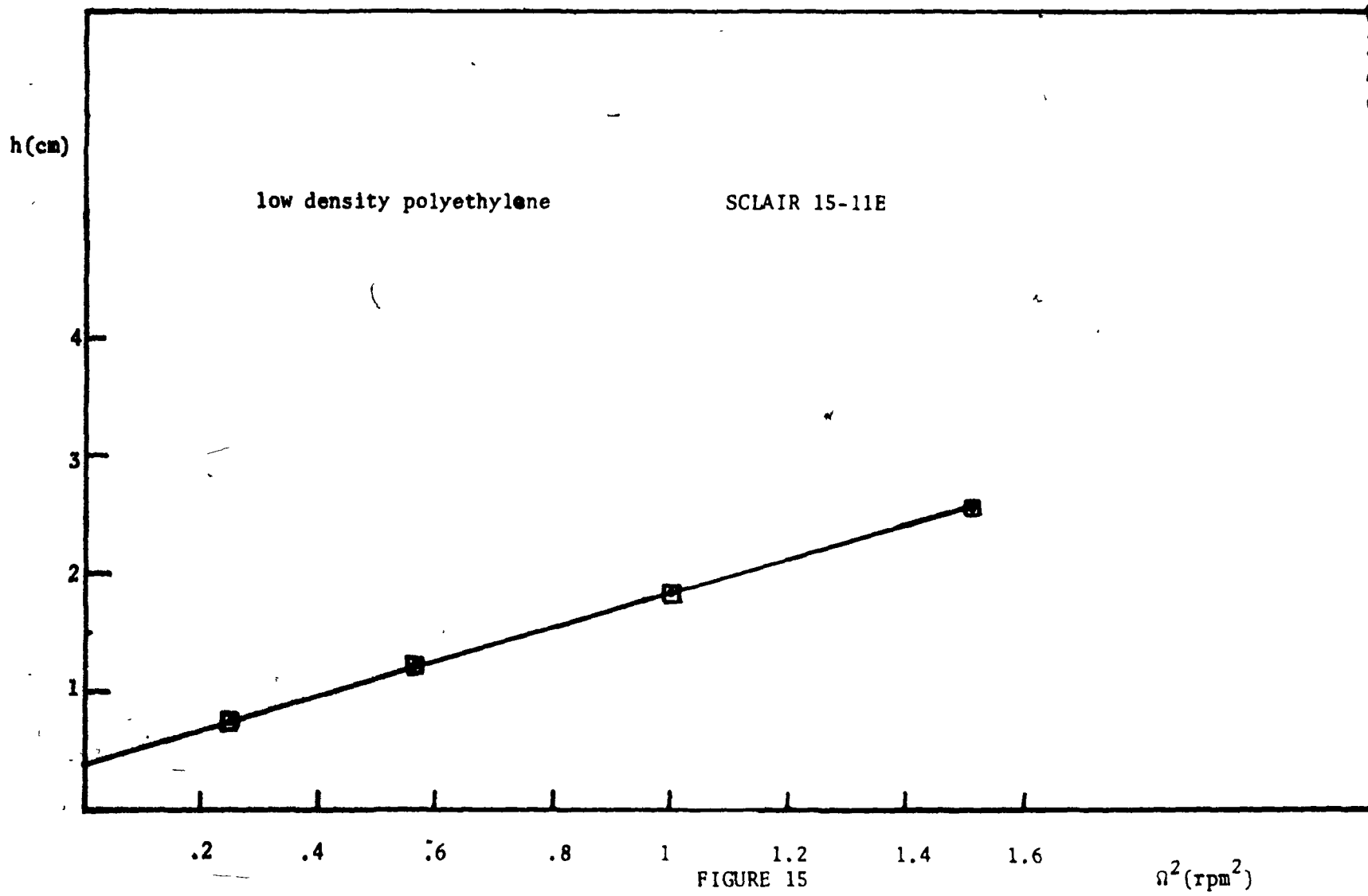


FIGURE 16. Viscosity versus Shear Rate Curve for Resin 4

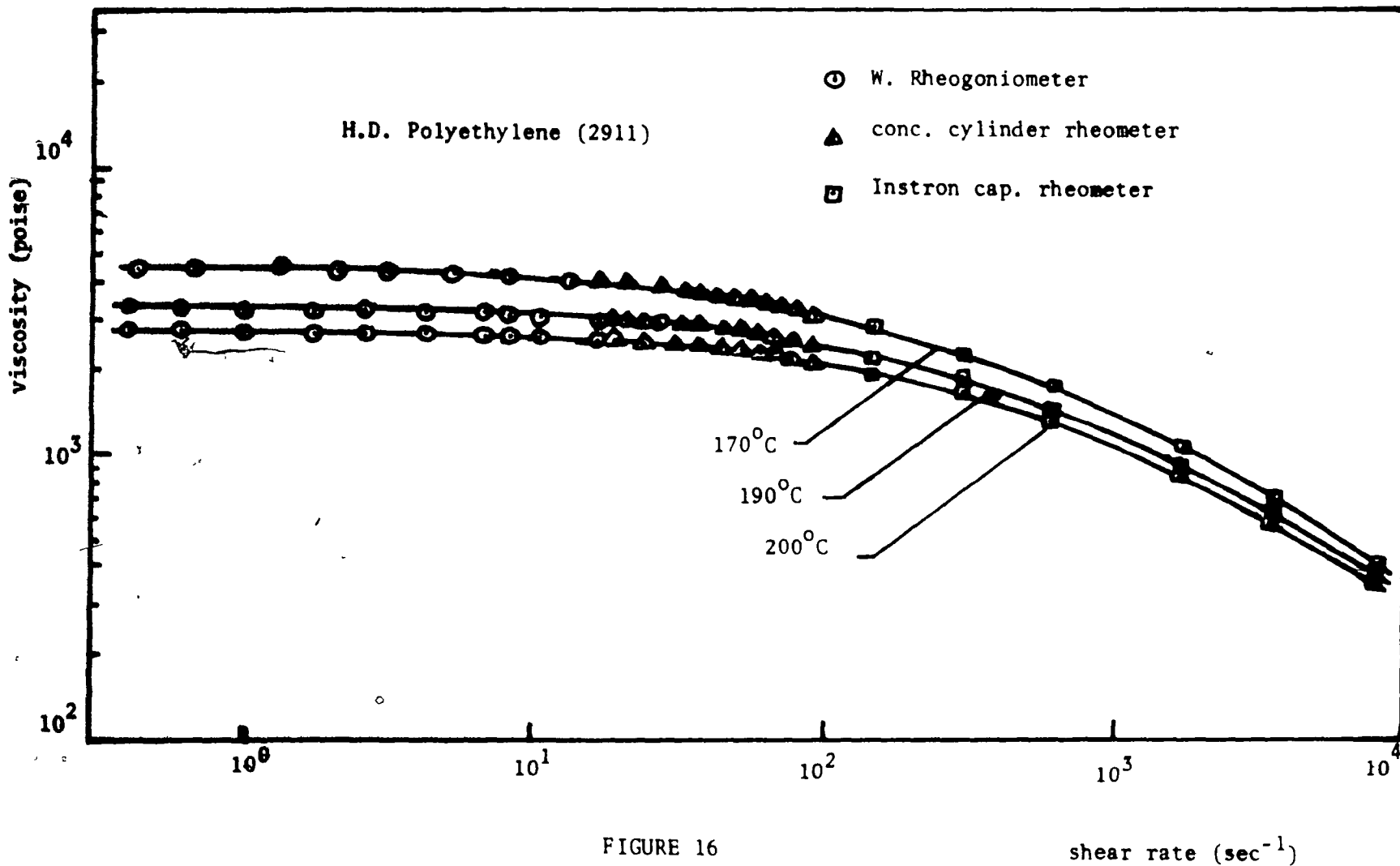


FIGURE 16

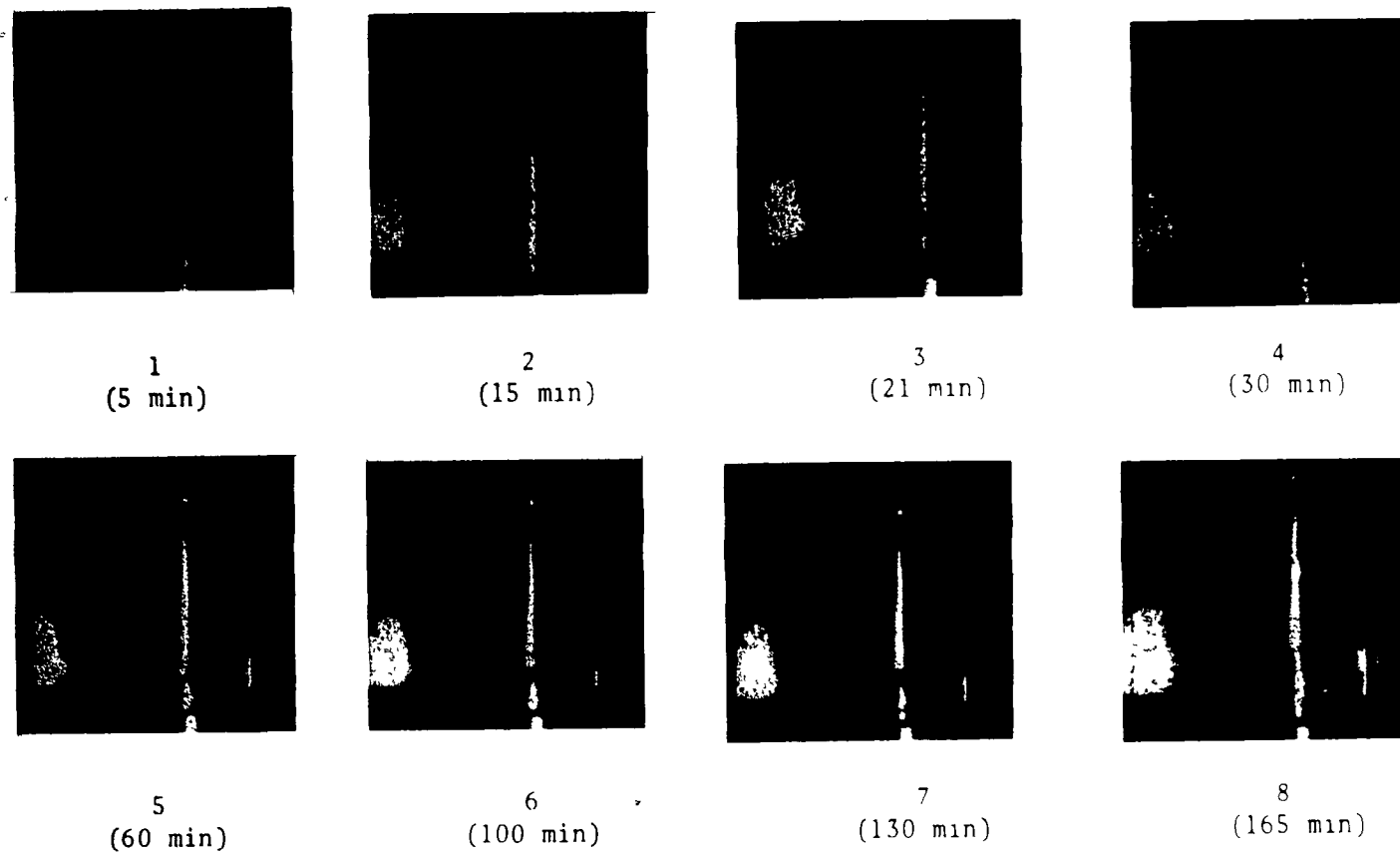


FIGURE 17. The Shape of the Free Surface at Various Angular Velocities ($\Omega = 5, 7.5, 10, 12.5, 15, 20, 25, 40$ rpm, respectively)

FIGURE 18. Rise versus Angular Velocity Curve for Resin 4

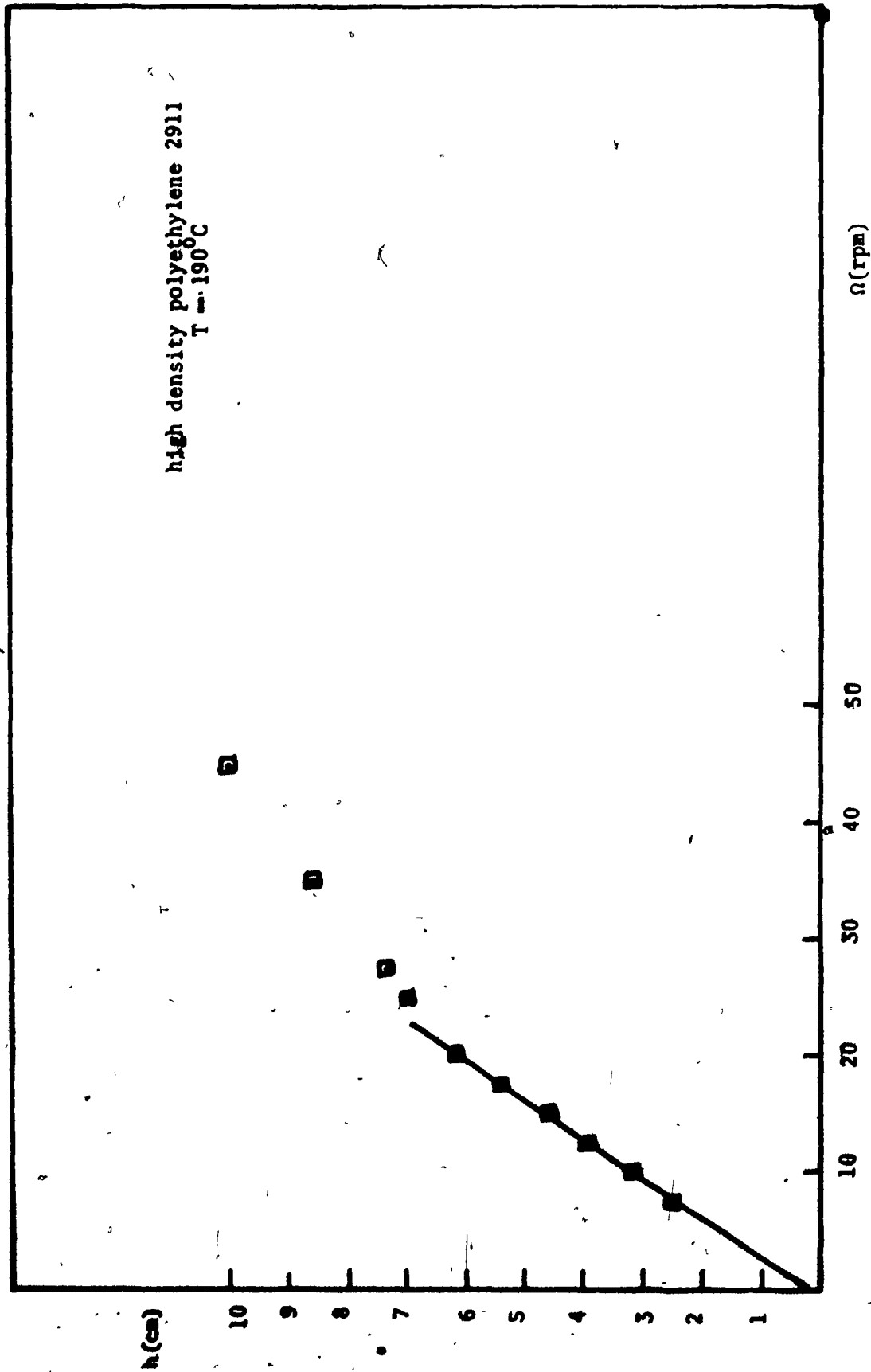


FIGURE 18

For low speed, the free surface assumes a concave shape. For higher speed, it assumes a convex shape. At $\Omega = 20$ rpm, some waves in the raised column are observed. It is the beginning of the instability. The graph of the height of rise versus the angular velocity (Fig. 18) shows that, before the point of instability, the height varies linearly with the angular velocity.

Discussion of Results

The experimental results indicate that the height of rise is higher when the viscosity is higher and when the density is lower. This is what might have been expected. Indeed, usually, a polyethylene which has a higher viscosity and lower density, is more highly branched and more elastic, and the first normal stress difference is greater, resulting in a higher climb. Hence, by simply observing the height of rise of two polymer melts submitted to the flow near a rotating rod, one might be able to get some idea of the relative order of magnitude of the viscosity (and the density) of these polymers.

Some other observations can be drawn from the experimental results:

-The steady state is reached more rapidly for a less viscous polymer.

-From the curves of h versus time, for the two LDPE, we notice that these two resins behave similarly; for higher speed, the height increases rapidly at the beginning, then there is a period of time in which it keeps a constant value, and then it increases again, to reach finally a steady state. The period of constant height or nearly constant height is longer for the resin with higher viscosity (resin 10). If we

look at Figs. 11 and 15 (curves of h versus time for resins 10 and 1, respectively), we notice that for resin 1, the second rise, relative to the first, is greater for higher speed, whereas for resin 10, the contrary is observed. However, this fact cannot be generalized, since, if we did for resin 10 some experiments with rotational speeds between .5 and .75 rpm and for resin 1 some experiments with rotational speeds higher than the highest speed studied, we might observe that the two resins behave in the same way, i.e. the relative height of the second rise might increase with the speed at the beginning, attain a maximum, and then diminish.

The bifurcation observed for the two LDPE's is a very complex phenomenon which cannot be explained completely. From the time $t = 0$, to the time when the period of constant height obtains, a rational explanation may be given: at the beginning, the normal stresses, greater than the gravity force, force the polymer up along the rod. The rise is rapid in this stage. When the normal stresses are balanced by the gravity, the height can no longer increase. However, polymer continues to be drawn from the main body of the melt to the rod, and forced to climb it. Since the height cannot increase, the polymer which climbs up will enlarge the top of the raised column which falls down under the gravity force. This mechanism occurs very slowly because of the high viscosity of the melt, until every fluid element in the column reaches its equilibrium state. Then the height increases again. One may interpret this phenomenon by stating that the first equilibrium state is unstable, so that a new rise occurs to arrive at a final equilibrium state.

For the variation of the height of rise with the angular velocity, if the experimental results obtained in this work are compared with the theoretical results of Joseph, Fosdick and Beavers (7), who stated that the height of rise was proportional to the square of the angular velocity, one finds that only one of the resins studied behaves according to this theory. Hence, the second-order theory developed by Joseph et al. does not apply in general to polymer melts, nor can the "fluid of grade 2" and the "fluid of grade 4". To fully describe the mechanism involved in the Weissenberg effect in polymer melts, a more complete constitutive equation must be employed.

CHAPTER IV

CONCLUSIONS

The experimental work carried out in this study demonstrates that the polymer melts, like other viscoelastic fluids, exhibit the climbing phenomenon.

The results obtained regarding the influence of the viscosity and the density on the height of rise are those which may be expected: a higher viscosity (lower density) gives a higher height of rise.

It has been found that for the high density polyethylene, the height of rise varies linearly with the angular velocity, whereas for one of the two low density polyethylenes studied, the height is proportional to the square of the angular velocity. But the mechanism involved in the rod-climbing phenomenon of polymer melts is very complex, and more studies must be done if one wishes to arrive to a complete description of the phenomenon.

Regarding the apparatus used in this work, some points must be considered during the experimentation:

-Some care must be taken to avoid the oxidation of the melt. The climbing phenomenon is greatly affected by the oxidation. A uniform height of the glass cylinder, and a layer of silicone sealant fixed on the edge of the glass cylinder are very helpful.

-Because of the interstices between the polymer granules, the volume occupied by these granules will diminish when they are melted, resulting in a considerable wetting at the wall of the glass cylinder,

so that the visibility of the free surface is very bad, and photographs cannot be taken. To avoid this situation, when the polymer granules are poured into the glass tube, one must take care to eliminate the contact of these granules with the wall of the glass cylinder at the side from which photographs will be taken. Even though, there is still some wetting due to surface tension, which makes more or less difficult the determination of the exact horizontal surface of the melt.

-Some difficulties may arise if one wants to do experiments with higher speeds for resin 10, since the window through which photographs were taken is not sufficiently large.

BIBLIOGRAPHY

1. Beavers, G.S. and D.D. Joseph, "The Rotating Rod Viscometer", J. Fl. Mech., 69, 475 (1975).
2. Chan, LL.-Y., "Experimental Observations and Numerical Simulation of the Weissenberg Climbing Effect", Ph.D. Thesis, Univ. of Mich., 1972.
3. Chezeaux, M., "Sur les Fluides Présentant l'Effet Weissenberg", Journ. de Mecanique, 10, 224 (1971).
4. Garner, F.H., A.H. Nissan, and Jack Walker, "Normal Stresses in Sheared Viscoelastic Systems", I.E.C., Vol.51, No.7, 858 (1959).
5. Hoffmann, A.H. and W.G. Gottenberg, "Determination of the Material Functions for a Simple Fluid from a Study of the Climbing Effect", Trans. Soc. Rheol., 17, 405 (1973).
6. Joseph, D.D., G.S. Beavers, and R.L. Fosdick, "The Free Surface on a Liquid between Cylinders Rotating at Different Speeds", Archive for Rational Mechanics and Anal., 49, 381 (1973).
7. Joseph, D.D. and R.L. Fosdick, "The Free Surface on a Liquid between Cylinders Rotating at Different Speeds", Archive for Rational Mechanics and Anal., 49, 321 (1973).
8. Kaye, A., "The Shape of a Liquid Surface between Rotating Concentric Cylinders", Rheol. Acta., 12, 206 (1973).
9. Kündu, P.K., "Normal Stresses and the Weissenberg Effect", Trans. Soc. Rheol., 17, 343 (1973).
10. Oldroyd, J.G., "Non-Newtonian Effects in Steady Motion of some Idealized Elastico-viscous Liquids", Proc. Roy. Soc., A245, 278 (1958).
11. Saville, D.A. and D.W. Thompson, "Secondary Flows Associated with The Weissenberg Effect", Nature, 223, 391 (1969).
12. Truesdell, C., "The Elements of Continuum Mechanics", Springer-Verlag. New York, Inc., New York (1966).
13. Weissenberg, K., "A Continuum Theory of Rheological Phenomena", Nature, 159, 310 (1949).

NOMENCLATURE

<u>Symbol</u>	<u>Definition</u>
a	radius of the rotating rod
$A_{ij}^{(1)}$	component of the first Rivlin-Erickson tensor
$A_{ij}^{(2)}$	component of the second Rivlin-Erickson tensor
h	height of rise
p	isotropic pressure
P_{ij}	component of the stress tensor
r	radius
(x_i, x_j, x_k)	rectangular Cartesian co-ordinates
v_i, v_j, v_k	components of the velocity vector
$\alpha_1, \alpha_2, \hat{\beta}, \nu$	material constants
ρ	density
δ_{ij}	Kronecker delta
Ω	angular velocity